Cation removal behaviour by cross-linked sodium alginate-PVA beads: characterisation, kinetics and equilibrium studies.

N. Flores-Alamo[a], M.J. Solache-Rios[b], C.G. Aguirre-Malvaez[a], F. Cuellar-Robles[a], M.C. Carreño-De León[a],*

[a]*División de estudios de Posgrado e Investigación, Instituto Tecnológico de Toluca, Av. Instituto Tecnológico S/N, S/N, Colonia Agrícola Bellavista, Metepec, Estado de México, C.P. 52149, México, Tel. +(52)722 2 08 72 18; emails: mcarrenod@toluca.tecnm.mx (M.C. Carreño-De León), nfloresa@toluca.tecnm.mx (N. Flores-Alamo), caguirrem@toluca.tecnm.mx (C.G. Aguirre-Malvaez), fcuellarr@toluca.tecnm.mx (F. Cuellar-Robles)*
[b]*Departamento de Química, Instituto Nacional de Investigaciones Nucleares, D.F., C.P. 11801, Apdo, Postal 18-1027, Mexico, email: marcos.solache@inin.gob.mx (M.J. Solache-Rios)*

ABSTRACT

Novel adsorbent materials were prepared from sodium alginate and polyvinyl alcohol (AL-PVA) in 5 different ratios to evaluate their adsorption capacities for Pb(II), Cu(II) and Zn(II) in a multicomponent solution of 10 mg/L of each metal, then they were tested with wastewater from a glass industry to remove these heavy metals. The adsorption tests with the materials of different AL-PVA ratios showed that the most efficient material was the one with the ratio 50/50, this composite was characterized by SEM and FTIR spectra before and after the adsorption process; the zero-point charge, swelling kinetics and acid resistance tests were determined. The experimental multicomponent adsorption kinetics data fitted best the pseudo-first-order model according to the R^2 values and the similarity between the experimental adsorption capacity and the calculated one, the adsorption isotherm data of Pb(II) fitted best to the linear model and those of Cu(II) and Zn(II) to the Langmuir model. The adsorbent material shows a high potential for the removal of Pb(II), Cu(II) and Zn(II).

Keywords: Adsorption; Multicomponent; Physisorption; Chemisorption; Freundlich

1. Introduction

Currently, there is a great concern worldwide on the increasing rates of industrial effluents contamination by heavy metals. Common heavy metal pollutants are Cd, Cr, Hg, Pb, Cu, Zn and As. Environmental pollution with these metals has been accelerated in modern society due to industrialisation, population growth and overexploitation of natural resources.

The glass industry includes a variety of manufacturing products. It produces glass objects from a wide range of raw materials among them the most important ones are silica sand, glass cullet, and intermediate/modified materials such as soda ash, limestone, dolomite, and feldspar, the highest quantity of water is used during cooling and cullet cleaning [1,2]. Metal emission is an important issue in some sub-sectors (e.g., lead crystal and frits production); however, this problem is present in all other glass manufacturing sectors to a lesser degree. Heavy metals may be present as minor impurities in some raw materials, in cullet, and in fuels. Lead and cadmium are used in fluxes and coloring agents in the frit industry. Particles from lead crystal manufacture may have a lead content of 20%–60%. Special glass manufactures may release arsenic, antimony, and selenium (the

coloring agent in bronze glass or decoloring agent in some clear glasses). The chemicals used for coloring glasses are mainly the metallic oxides. The heavy metals dissolved into the water when the equipment and the floor of the factory are cleaned [2].

Heavy metals enter food chains from contaminated soil, water and air, causing pollution and significant adverse health effects in invertebrates, fish and humans [3,4]. Lead is one of the most common and toxic heavy metal widely used in industrial activities such as metal plating, petroleum refining, battery manufacturing, smelting, mining and painting [5]. Serious health problems occur when lead concentrations are high, lead poisoning can cause kidney damage, anaemia and symptoms of toxicity including impaired kidney function, hypertension and headache [6].

Copper contamination is caused by the manufacture of printed circuit boards, metal finishing industry (pickling of copper and its alloys), electroplating and electrical polishing, paint manufacture, wood preservatives and printing operations [7]. Copper maybe incorporated into various humans' enzymes, excess of Cu(II) causes extensive damage to eyes and liver and imbalance in cellular processes that cause Menkes, Wilson's, Alzheimer's, Parkinson's and prion diseases [8].

Zinc plays a key role for several important biological processes in the human body [9], it is necessary for the functioning several enzyme systems, deficiency of zinc leads to growth retardation and anaemia, a condition known as "zinc deficiency syndrome". Symptoms of zinc toxicity in humans include vomiting, dehydration, electrolyte imbalance, abdominal pain, nausea, lethargy, dizziness and lack of muscle coordination [10].

Various treatment methods such as reverse osmosis, adsorption, precipitation, coagulation, evaporation, oxidation/reduction, ion exchange, electrolysis, magnetic separation, among others have been used to remove these metals, however, some methods are often ineffective and expensive at low concentrations in solution, and have disadvantages like high reagents use, high energy requirements and production of toxic secondary sludges [11].

Adsorption is widely used in the wastewater treatment processes to remove pollutants from water because this technique is simple, efficient, and economically viable [12].

Recently, one of the bio-based materials used as an adsorbent for heavy metals is sodium alginate, because it is abundant in the algae of the ocean, due to gelling ability of alginate, alginate beads, formed by adding mostly calcium, were used for heavy metal removal and they have received attention as adsorbents for heavy metals removal from wastewater due to its biodegradability, hydrophilicity and abundance in nature. In addition, the presence of carboxylate (COOH) groups provides the ability to form complexes with a variety of multivalent ions [13]. Recent studies were particularly focused on improvement of alginate beads by adding some materials capable of capturing heavy metals or improve their mechanical an thermal stabilities, like polyvinyl alcohol, it is a semi-crystalline polymer, soluble in water and suitable for combining with other polymers to increase physical and thermal stability properties [14].

The main objective of this research was to determine the removal efficiencies of Pb(II), Cu(II) and Zn(II) from a multicomponent solution and from a wastewater from a glass industry, using a material obtained from sodium alginate-polyvinyl alcohol cross-linked with $CaCl_2$. In addition, the characterisation of the material was performed by FTIR, SEM, pH-zpc, swelling kinetics and acid resistance tests. The adsorption tests were performed in the batch system, considering the effect of pH on the adsorption capacity of each metal ion present in solution, adsorption data were treated with the pseudo-first-order and pseudo-second-order models for the kinetics and the Langmuir, Freundlich and linear models for the isotherms.

2. Materials and method

2.1. Materials

Meyer brand México pure sodium alginate (AL) molecular weight of 216 g/mol, Meyer brand polyvinyl alcohol (PVA) with a concentration of 95%–100%, and Jalmek brand México calcium chloride anhydrous molecular weight of 110.98 g/mol were used for the preparation of the adsorbent material, and copper (nitrate), lead (sulphate) and zinc (sulphate) Golden Bell brand standards with a concentration of 1,000 mg/L each one were used for the adsorption process. Meyer brand nitric acid with a concentration of 68%–70% and molecular weight of 63.01, sodium hydroxide pellets molecular weight of 40 g/mol and J.T. Baker brand sulphuric acid ACS Reagent molecular weight of 98 g/mol and hydrochloric acid concentration of 36.5%–38% molecular weight of 36.46 g/mol and deionised water were used for the preparation of solutions.

The solution used for the experiments involving the adsorption of heavy metals was prepared as a multicomponent aqueous solution at a concentration of 10 mg/L of each metal from standard solutions of Pb(II), Cu(II) and Zn(II). Wastewater from a glass industry was used for adsorption kinetics experiments and partial isotherm tests, this wastewater coming directly from the cooling and washing process did not present considerable apparent fouling as floating particulate matter, so it was only subjected to an acidification process (pH 5) and sedimentation for a period of 24 h in imhoff cones before it was used, and it was kept at a temperature of 4°C. The concentrations of the heavy metals determined in the wastewater were Pb(II) 0.18 mg/L, Cu(II) 1.72, and Zn(II) 4.63 mg/L.

2.2. Preparation of the adsorbent material

The material was prepared with 5 different ratios (100/0 (1), 75/25 (2), 50/50 (3), 35/65 (4) and 25/75 (5) %w/w) from AL (1%) and PVA (7.7%) solutions. The 7.7% w/w PVA solution was prepared with deionised water with constant stirring at 500 rpm for 2 h and 70°C under continuous refluxing and the 1% w/w AL solution was prepared with constant stirring at 500 rpm for 24 h and a temperature of 65°C. The solutions were mixed and dripped into a 0.1 M $CaCl_2$ solution using a peristaltic pump connected to a 0.9 mm hypodermic needle, the beads were left to mature 24 h at 300 rpm, and finally the beads were washed with distilled water to remove the excess of $CaCl_2$ and dried in the oven at 25°C for 48 h.

2.3. Effect of AL/PVA ratio on ion removal of cations

Individual solutions of each metal ion (Pb(II), Cu(II) and Zn(II)) were prepared at a concentration of 10 mg/L, the solutions were adjusted to pH 5, then approximately 0.5 g (weighed to four significant figures) of wet beads of different ratios of AL-PVA were placed in 10 mL of metal ion solution, the mixtures were shaken for 24 h at 25°C. At the end of the stirring time, the remaining concentrations of Pb(II), Cu(II) and Zn(II) in the solutions were determined by atomic absorption spectrometry using a Perkin Elmer Model Analyst 200 spectrophotometer at wavelengths (λ) of 216.8, 327.4 and 213.9 nm for Pb(II), Cu(II) and Zn(II) respectively. The removal percentages were determined by the following equation [15]:

$$\%\text{Removal} = \frac{(C_o - C_t)}{C_o} \times 100 \tag{1}$$

where C_o is the initial concentration of each ion (mg/L) and C_t is the concentration at time t (mg/L) [13].

2.4. Characterisation of the adsorbent material

The material that showed the highest removal capacity was selected and characterized by swelling kinetics, scanning electron microscopy (SEM), Fourier transform infrared spectroscopy (FTIR), acid resistance test and point of zero charge (pH-zpc). Individual solutions of the metals were used to saturate the material with each metal and analyse them by SEM and FTIR.

2.5. SEM and FTIR analysis

A JEOL JSM-6610LV electron microscope was used at 20 kV using EDS, the sample was placed on a double-sided electrically conductive carbon tape and was gold plated for 30 s to improve the conductivity of the sample. To perform the EDS analysis, the beads were saturated with individual solutions of Pb(II), Cu(II) and Zn(II)), to corroborate that the adsorption process of metals took place.

A Fourier transform infrared (FTIR) analysis was carried out by using a Varían spectrophotometer, model 640, operated at wavenumber intervals from 400 to 4,000 cm^{-1} to determine the presence of the functional groups in the adsorbent material after the adsorption processes.

2.6. Swelling kinetics

To evaluate the water retention capacity of the adsorbent material, approximately 0.5 g (weighed to four significant figures) of beads were placed in distilled water, with constant stirring of 200 rpm [16] different times (from 0 to 160 min), then the beads were removed from the water, placed on filter paper to remove the excess of water and then weighed. Once the weight was recorded, the adsorbent material was returned to the container and the same procedure was repeated until the weight of the beads remained constant. The amount of water adsorbed by the beads was expressed as percentage and was determined by using the following equation:

$$\%\text{Swelling} = \frac{W - W_o}{W_o} \times 100 \tag{2}$$

where W is the weight of the beads at different times (g) and W_o is the initial weight of the beads (g).

2.7. Point of zero charge (pH-zpc) and acid resistance

The experiments were carried out in aqueous solution at different initial pH (pH$_{ini}$) values between 3 and 10 (pH was adjusted with diluted NaOH or HNO$_3$ solutions). For this purpose, approximately 0.5 g of beads were weighed and placed in contact with 10 mL of 0.1 M NaNO$_3$ solutions of different pH, at constant stirring of 200 rpm for 1 h at room temperature (25°C) and at the end of this time, the final pH in the solutions was measured. Finally, pH$_{ini}$ vs. DpH (pH$_{ini}$ – pH$_{fin}$) was plotted, the pH-zpc corresponded to the intersection between curve and the abscissa axis.

To determine the stability of the adsorbent material and possible dissolution, approximately 0.5 g of wet beads were placed in contact with 10 mL of acidic solutions of HCl, HNO$_3$ and H$_2$SO$_4$ at pH 1, 2 and 4, the samples were kept under constant stirring at 200 rpm for 48 h at room temperature (25°C).

3. Batch adsorption tests

The adsorption processes were evaluated with AL-PVA beads (ratio 3, 50/50), considering the effect of pH on the adsorption capacity, kinetics and isotherms.

3.1. Effect of pH on adsorption capacity

To determine the optimum pH for the highest adsorption capacity, a multicomponent solution of the metal ions was prepared (10 mg/L of each one) and adsorption tests were carried out at different pH of the solution between 3 and 8, using approximately 0.5 g of beads in 15 mL of solution with a constant stirring for 24 h at 25°C. Finally, the remaining concentration of each ion in the solution was determined by using atomic absorption spectrophotometry at the wavelength corresponding to each ion and the percentage of removal was calculated by Eq. (1).

3.2. Adsorption kinetics

For adsorption kinetics experiments, approximately 0.5 g of wet beads were placed in contact with 15 mL of a multi-component solution of the metal ions (10 mg/L of each one) adjusted to the optimum pH value of 5.5, then the samples were placed in agitation different times (0.25, 0.50, 0.75, 1, 2, 4, 6, 8 and 24 h), 3 runs were carried out at temperatures of 25°C, 40°C and 50°C, then the remaining concentrations were determined as described above and the adsorption capacities were calculated considering dry weight (Eq. 3), the experimental data were adjusted to the optimum pH value of 5.5 with diluted NaOH or HNO$_3$ solutions [17]. The experimental data were fitted to the pseudo-first-order [Eq. (4)] and pseudo-second-order [Eq. (5)] kinetic models by using the Origin software [18].

$$q_t = \frac{(C_o - C_e) \cdot V}{w} \quad (3)$$

where C_o is the initial concentration of each ion (mg/L), C_e is the equilibrium concentration of each ion (mg/L), V is the volume of the solution (L), w is the weight of the beads on dry basis (g).

$$q_t = q_e \left(1 - e^{k_1 \cdot t}\right) \quad (4)$$

$$q_t = \frac{k_2 q_e^2 \cdot t}{1 + k_2 q_e \cdot t} \quad (5)$$

where q_t is the amount of metal adsorbed over time (mg/g), q_e the amount of metal adsorbed at equilibrium (mg/g), k_1, k_2 are the pseudo-first-order and pseudo-second-order kinetic constants respectively and t is time (min).

A similar procedure was carried out at 25°C using wastewater obtained from an effluent of a glass industry, the contact times were 5, 15, 30, 45, 60 min, 2, 3, 4 and 5 h. In this effluent, the concentrations of Pb(II), Cu(II) and Zn(II) were previously determined by using atomic absorption spectrophotometry.

3.3. Adsorption isotherms

Approximately 0.5 g of wet beads were placed in contact with 15 mL of the multicomponent solutions with concentrations ranging from 2 to 300 mg/L of each ion, the samples were placed under constant stirring for 8 h in three runs at temperatures of 25°C, 40°C and 50°C. The remaining concentrations of each metal in the solutions were determined and the adsorption capacities at equilibrium were calculated, the results for each ion were individually fitted to the linear (Eq. 6), Langmuir [Eq. (7)] and Freundlich [Eq. (8)] models [15].

$$q_e = m \cdot C_e \quad (6)$$

$$q_e = \frac{q_{max} b \cdot C_e}{1 + b \cdot C_e} \quad (7)$$

$$q_e = k_F \cdot C_e^{1/n} \quad (8)$$

where q_{max} is the maximum adsorption capacity (mg/g), C_e is the concentration of each ion at equilibrium (mg/L), b, k_F and n are constants.

4. Results and discussion

4.1. Effect of AL-PVA ratio on the removal of metal ions

Fig. 1 shows the removal percentages for each ion, for Pb(II) a maximum removal of 98% was obtained with AL-PVA 50/50 (3), slightly higher than the percentage obtained with the other ratios. For Cu(II), the highest
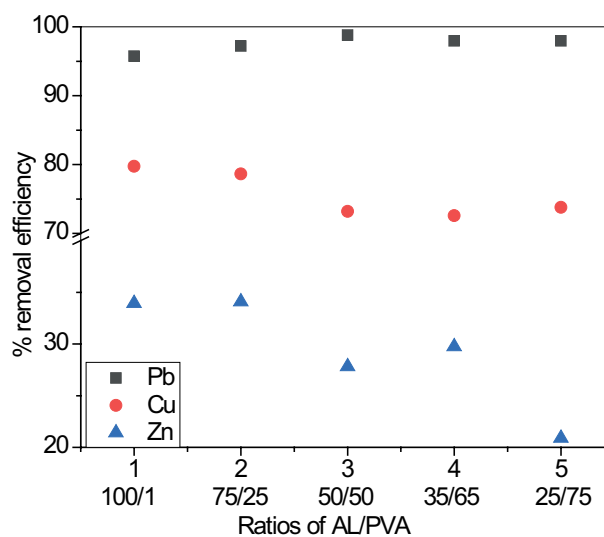
Fig. 1. Removal percentages for (a) Pb(II), (b) Cu(II) and (c) Zn(II) by AL-PVA of different ratios.

removal was 80% with ratio 1 and for Zn(II) the highest removal was 34% with ratio 2. The selectivity of the material for the removal of each ion was Pb(II) > Cu(II) > Zn(II), similar results were reported by [19]. Considering the toxicity of each ion, Pb(II) removal was prioritised and AL-PVA 50/50 ratio 3 was chosen as the optimum material for subsequent adsorption experiments.

4.2. Characterisation of the adsorbent material

4.2.1. SEM and FTIR analysis

The micrographs show a general view of the beads with an average diameter of 2 mm with a smooth surface morphology (Fig. 2a), with surface sections apparently formed by fiber-like yarns, possibly due to the crosslinking of the polymers used (Fig. 2b).

The micrographs of Fig. 3 correspond to the material of 50/50 ratio, at a magnification of 500 X a rough and slightly porous and irregular surface of the material is observed at 3,000 X, the average size of the pores observed was 2 mμ, with approximately 1 pore per 10 mμ².

To determine the elemental analysis of the adsorbent material and to corroborate the presence of metal ions after the adsorption processes, an analysis by SEM-EDS was performed. The results are shown in Table 1, the material is mainly composed of carbon, oxygen, calcium, in addition to the presence of Pb, Cu and Zn, which indicates the interaction between the adsorption sites of the material and the ions.

4.2.2. Swelling kinetics

The swelling percentage increases as the amount of PVA increased (ratios 4 and 5), reaching values of 400% (Fig. 5) in 2 h, the swelling capacity depends on the groups present in the structures, such as –OH [20] and PVA is a polymer that has a high capacity to absorb water due to its hydrophilic nature [21], but the beads were broken easily.
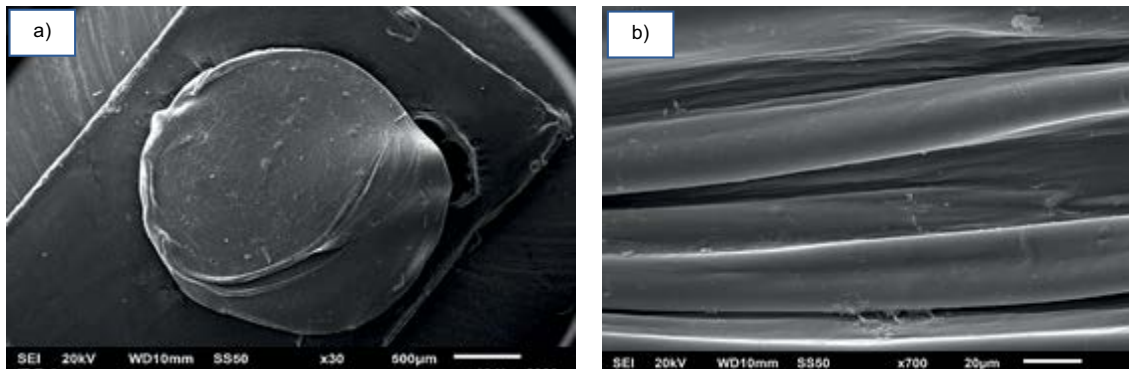
Fig. 2. Micrographs of the bead at (a) 30X and (b) 700X.
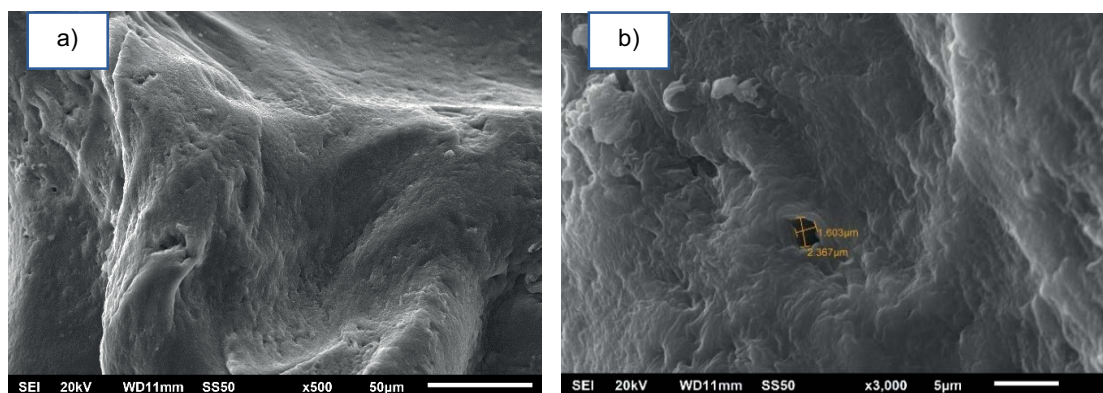
Fig. 3. Micrographs of beads of the 50/50 AL/PVA ratios.

Table 1
Elemental analysis of AL/PVA (50/50) by EDS after adsorption

Element	%w	%w	%w
C	43.16	42.63	44.46
O	52.53	49.91	47.82
Ca	2.28	3.67	4.24
Pb(II)	2.03		
Cu(II)		3.79	
Zn(II)			3.48

Ratios 1, 2 and 3 follow the same trend; the swelling percentage increased as the amount of PVA increased and the times to double their sizes were long, 120, 100 and 40 min respectively, so the beads of ratio 3 reached that percentage in less time, moreover, the bead retained its shape.

4.2.3. Fourier transform spectroscopy (FTIR)

The Fourier transform infrared spectra of AL-PVA beads 50/50 (3) ratio before and after the adsorption process by using single solutions of Pb(II), Cu(II) and Zn(II) are shown in Fig. 4.

The peak at 3,297 cm^{-1} decreased in intensity and the band shifts after adsorption of each ion, this peak corresponds to the –OH functional group which is attributed to

the ability to form complexes with the metal ions, the band at 2,921 cm^{-1} corresponds to stretching vibration of C–H bonds [22]. The bands at 1,606 and 1,400 cm^{-1} are due to asymmetric and symmetric COO stress vibration respectively, it is observed that both bands for the Cu(II) and Zn(II) ions are shifted and decrease in intensity, something similar occurs with the band at 1,080 cm^{-1} which corresponds to C–O–C vibration [23]. On the other hand, the 823 cm^{-1} band is assigned to the C–C stretching vibration of the polyvinyl alcohol. Finally, the presence of two bands around 1,245 and 617 cm^{-1} is related to the C–C stretching bond and possibly to effects of the Cu–O stretching vibration band which is attributed to the interaction of Cu(II) with surface –OH groups respectively [19]. For some other cations (Larkin, 2011) the bands identified with metal oxides ranged from 200 to 800 cm^{-1} and may be likely to be unappreciable.

4.2.4. Zero point charge (pH-zpc)

Fig. 6 shows the behaviour of the surface charge of the adsorbent material with respect to pH. A pH value of 6.6 was found to be the point of zero charge for the AL/PVA beads of ratio 3, above this value the surface charge of the material is negative due to the deprotonation of some carboxyl functional groups. This parameter was used to select the optimum pH value for the adsorption experiments of the ions in solution. It is observed that at pH values higher than 9 the adsorbent material dissolves in the solution, and
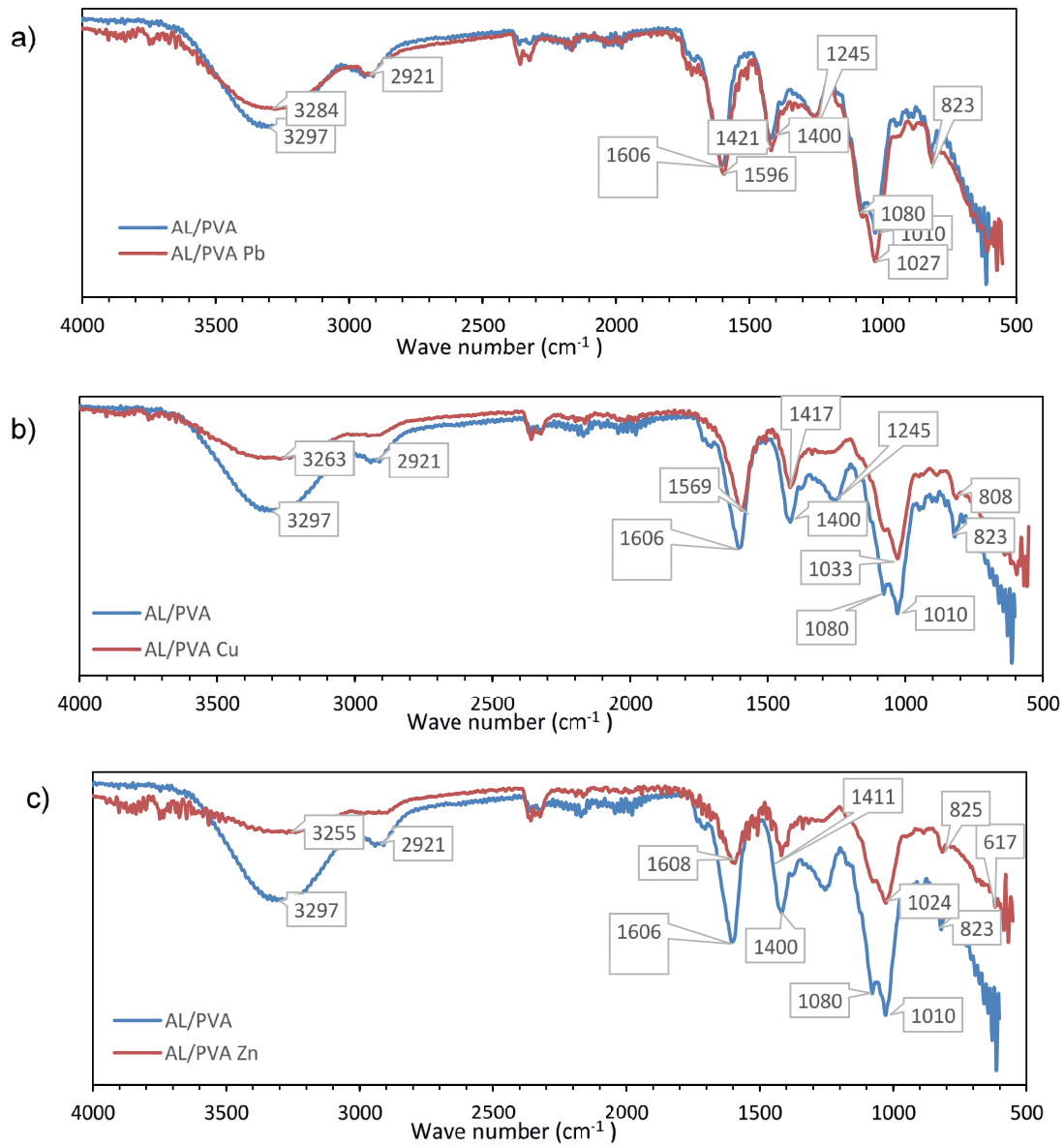
Fig. 4. IR spectra of AL/PVA (50/50 ratio) beads before and after adsorption of (a) Cu(II), (b) Pb(II) and (c) Zn(II).
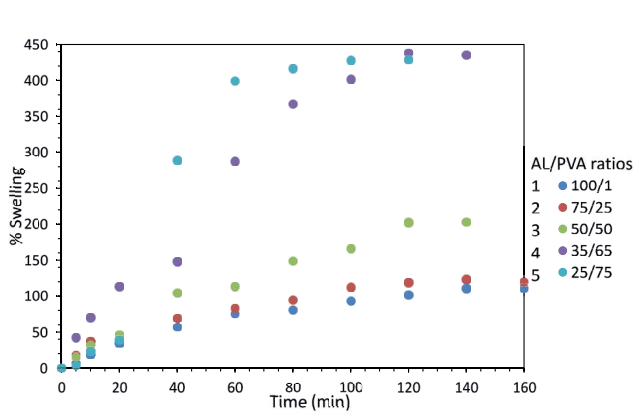
Fig. 5. Swelling of beads vs. time.
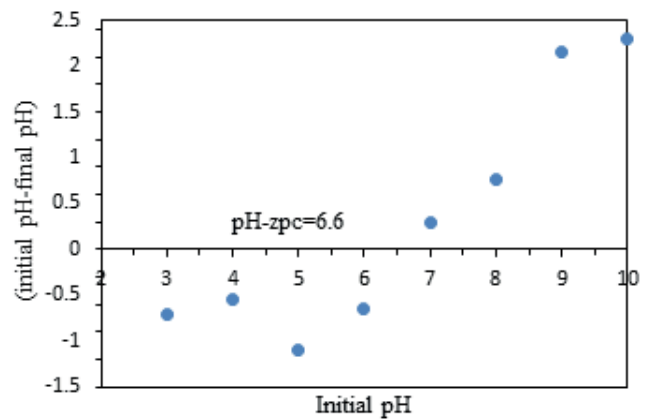
Fig. 6. Point of zero charge of AL/PVA bead ratio 3.

at values lower than 5 there may be a competition of the metal ions with the hydronium ions of the solution for the adsorption sites [24,25].

4.2.5. Acid resistance testing

The AL/PVA beads were apparently unstable at pH values of 1 and 2 (Table 2), in the case of HCl and H_2SO_4 at pH 1 there was fragmentation of the beads, so at pH 2 a significant weight loss was observed.

The most aggressive acid was H_2SO_4, at pH 1 and 2 the beads were fragmented and the least aggressive acid was HNO_3. At pH 4 the beads had a good stability and did not suffer any weight loss.

4.3. Adsorption tests in batch systems

4.3.1. Effect of pH on adsorption capacity

The adsorption behaviour using the multicomponent solution of 10 mg/L of each metal and the composite showed a removal efficiency of 100% for Pb(II) in a pH range from 3 to 8, for Zn(II) the increase of pH and removal percent was proportional, however at pH near 8 the precipitation of metal may take place. For Cu(II) the highest removal percent was achieved at pH 5 (Fig. 7). Considering the point of zero charge of 6.6 for the material, the pH of 5.5 was

Table 2
AL/PVA beads in acidic solutions

Acid	pH	% Weight loss	Fragmentation
	1	44	✔
HCl	2	38	
	4	0	
	1	49	
HNO_3	2	38	
	4	0	
	1	48	✔
H_2SO_4	2	48	✔
	4	0	

Fig. 7. Effect of pH on the removal of Cu(II), Zn(II) and Pb(II) by AL/PVA bead (ratio 3).

selected for the kinetic and isotherm experiments. Above pH 7, precipitation of Pb(II) as $Pb(OH)_2$ takes place and the adsorbent is not stable in basic conditions. The removal efficiencies for Pb(II), Cu(II) and Zn(II) obtained from glass industry wastewater were close to 59%, 85% and 32% at pH of 5.5, considering the initial concentrations: 0.23, 4.42 and 4.83 mg/L respectively. This behavior can be attributed to the different initial concentrations (Pb(II) 0.18 mg/L, Cu(II) 1.72, Zn(II) 4.63 mg/L) in the wastewater and the competition that may exist between them.

4.3.2. Adsorption kinetics

The adsorption kinetics data were fitted to the pseudo-first-order and pseudo-second-order models (Fig. 8). For Pb(II) the time to reach the equilibrium was about 1 h, however the contact time was longer to reach the equilibria for the other ions. For Cu(II) and Zn(II) the processes were slower around 2.5 h, the results show that the selectivity of the material for Cu(II) is the highest (3.57 mg/g at 25°C) then Pb(II) (2.59 mg/g) and finally Zn(II) (1.85 mg/g), possibly due to the ionic radii of Cu(II) of 0.69 Å; Pb(II) of 1.20 Å and Zn(II) of 0.74 Å, which could influence the accessibility to the active sites of the adsorbent material due to the steric hindrance, this behaviour is similar to that reported by [26]. For Pb(II), Cu(II) and Zn(II) at 25°C, 40°C and 50°C q_{exp} were 2.59, 2.53 and 2.53 mg/g, 3.57, 3.8 and 3.8 mg/g, 1.85, 2.04 and 2.13 mg/g, respectively for each heavy metal. The data shown in Table 3 indicate that the best fitting model was the pseudo-first-order model which suggests physical rather than chemical adsorption. The adsorption capacities (q_{exp}) decreased as the temperature increased (Table 3) for Pb(II) and Zn(II), the adsorption capacities increase as the temperature increase, this could be due to the ionic radius of Pb(II) which is greater than the radii of the other two ions. Although, the concentration of each metal in the solution was the same, the number of ions in that solution was different, being lower for Pb(II) than Cu(II) and Zn(II), 0.000048, 0.00016 and 0.00015 molar respectively.

For the glass wastewater, the kinetic parameters are shown in the Table 4, the experimental capacities (q_{exp}) for Pb(II), Cu(II) and Zn(II) were 1.08, 4.83 and 4.24 mg/g, respectively. A significant difference was observed between the adsorption capacities obtained for multicomponent solution (Table 3) and the wastewater from the glass industry (Table 4), this was attributed to the differences in the initial concentrations of each ion and the type of water. Kinetic experimental data were best fitted to pseudo-first-order for Pb(II) and Zn(II), and pseudo-second-order for Cu(II) according to the correlation factor (R^2) and experimental adsorption capacity.

When comparing the experimental adsorption capacity of each ion present in the multicomponent solution and the wastewater, differences in adsorption capacity are observed due to the difference in the initial concentration of each ion in the wastewater (Pb(II) 0.18 mg/L, Cu(II) 1.72, and Zn(II) 4.63 mg/L) in comparison to the multicomponent solution (10 mg/L for each), however the trend of q_{exp} for each ion is the same (q_{exp} Pb(II)<Cu(II)<Zn(II)). The difference in the initial concentrations of the wastewater may be the reason for achieving a fit lower to unity.
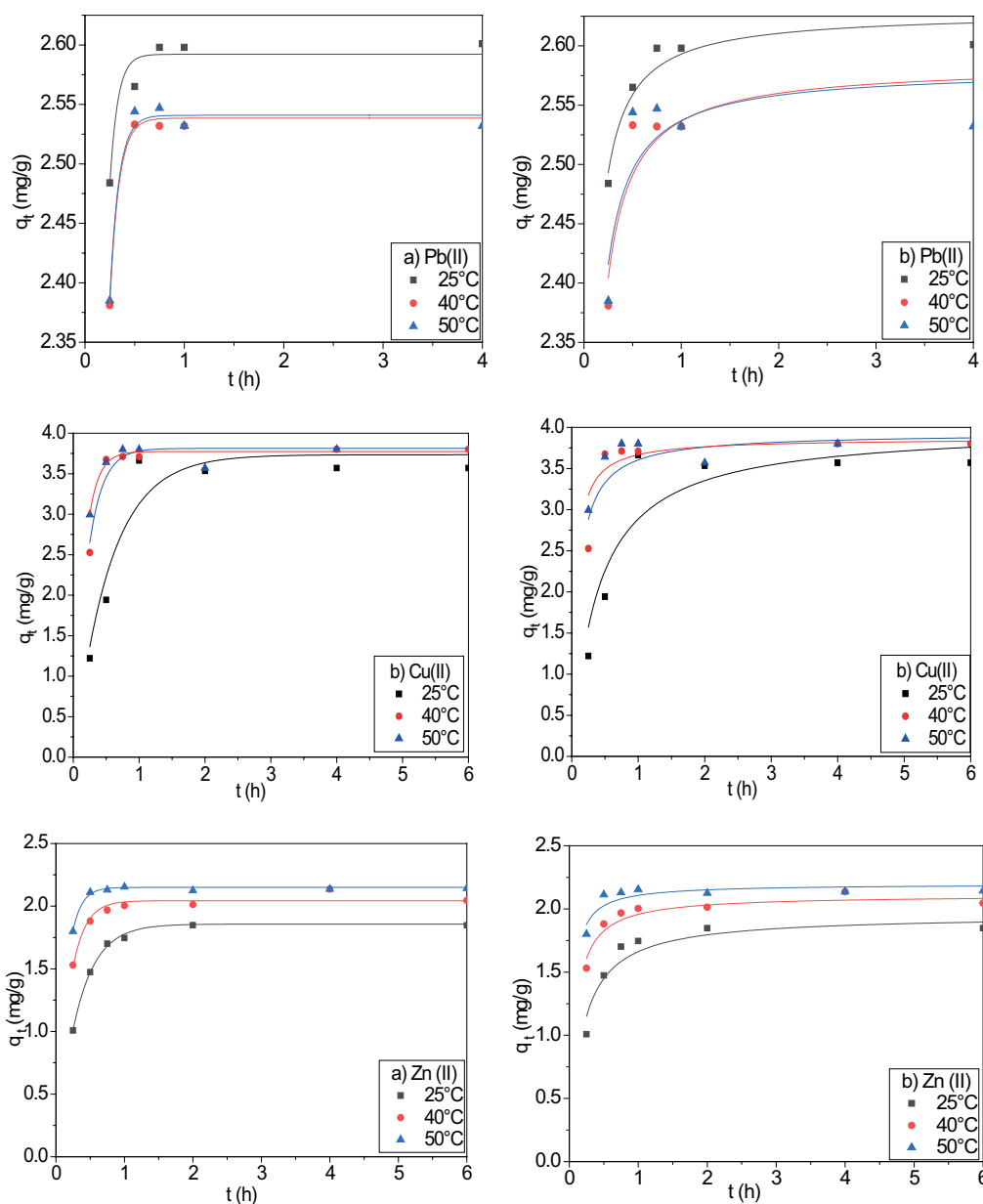
Fig. 8. Adsorption kinetics for Pb(II), Cu(II), Zn(II) in multicomponent solution fitted to the (a) pseudo-first-order and (b) pseudo-second-order model.

Table 3
Kinetic parameters for the adsorption of Pb(II), Cu(II) and Zn(II) in multicomponent solution by AL/PVA bead ratio 3

Pseudo-kinetic-model	T (°C)	Pb(II)			Cu(II)			Zn(II)		
		q_e	k	R^2	q_e	k	R^2	q_e	k	R^2
	25	2.59	12.63	0.92	3.72	1.81	0.92	1.85	3.14	0.99
Pseudo-first-order	40	2.53	11.13	0.99	3.81	4.75	0.94	2.04	5.35	0.95
	50	2.54	11.20	0.97	3.76	6.39	0.90	2.15	7.31	0.98
	25	2.62	1,340.75	0.90	4.00	165.63	0.84	1.95	42.72	0.90
Pseudo-second-order	40	2.58	924.89	0.78	3.93	668.31	0.71	2.10	120.46	0.88
	50	2.58	1,009.97	0.63	3.86	1,066.11	0.67	2.19	249.51	0.76

q_e (mg/g); k_1 (1/h) pseudo-first-order, k_2 (g/mg h) pseudo-second-order.

Table 4
Kinetic parameters for the adsorption of Pb(II), Cu(II) and Zn(II) from a glass wastewater industry

Pseudo kinetic model	T (°C)	Pb(II)			Cu(II)			Zn(II)		
		q_e	k	R^2	q_e	k	R^2	q_e	k	R^2
Pseudo-first-order	25	1.15	0.03	0.86	4.58	6.17	0.85	4.44	4.52	0.91
Pseudo-second-order	25	1.41	0.08	0.80	4.95	1,068.2	0.89	4.86	698.6	0.91

q_e (mg/g); k_1 (1/h) pseudo-first-order, k_2 (g/mg h) pseudo-second-order.
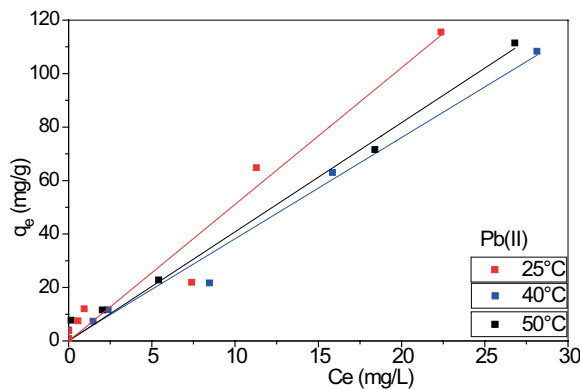
Fig. 9. Adsorption isotherm of Pb(II) in multicomponent solution fitted to the linear model.

4.3.3. Adsorption isotherms

Fig. 9 shows the experimental equilibrium data for Pb(II) fitted to a linear model, neither the Langmuir nor the Freundlich models were properly fitted, it is observed that the adsorption capacity and the metal concentration are directly proportional, C_e increases as q_e increases.

Table 5
Isotherm parameters for the adsorption of Pb(II) in multicomponent solution

	T (°C)	Slope	R^2
	25	5.11	0.96
Linear	40	3.80	0.99
	50	4.08	0.99

The parameters shown in Table 5 correspond to the linear model, the correlation coefficient is greater than 0.96 for all temperatures. Furthermore, it was observed as the temperature increases from 25°C to 40°C, the adsorption capacity decreases and then increases slightly at 50°C.

For Cu(II) and Zn(II) the experimental data at 25°C, 40°C and 50°C fitted the Freundlich and Langmuir models as shown in Fig. 10.

The parameters from the fitting of experimental data to the Freundlich and Langmuir isotherms models are presented in Table 6. The correlation coefficients for both metals are higher form the Freundlich than Langmuir model, this is because the shape of the isotherms is Freundlich type and indicates that the material is heterogeneous.
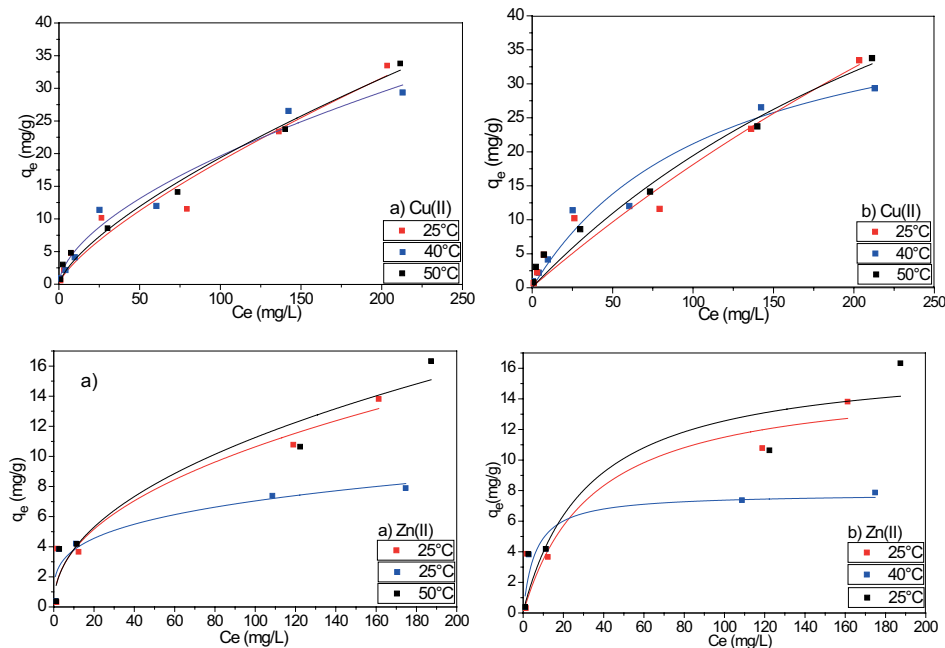
Fig. 10. Adsorption isotherms for Cu(II) and Zn(II) in multicomponent solution fitted to the (a) Freundlich and (b) Langmuir model.

Table 6
Isotherm parameters for the adsorption of Cu(II) and Zn(II) in multicomponent solution

		Freundlich			Langmuir		
	T (°C)	k_f^*	n	R^2	b^{**}	q_{max}	R^2
Cu(II)	25	0.61	1.34	0.95	1.3×10^{-3}	156	0.93
	40	1.35	1.72	0.97	8.7×10^{-3}	45.5	0.96
	50	0.77	1.43	0.98	2.8×10^{-3}	88.1	0.97
Zn(II)	25	1.35	2.23	0.92	0.03	15.4	0.86
	40	2.00	3.67	0.85	0.17	7.81	0.88
	50	1.31	2.14	0.92	0.03	16.6	0.86

*(mg/g)(L/mg)$^{1/n}$; **(L/mg).

Table 7
Adsorption capacities for Pb(II), Cu(II) and Zn(II) in wastewater from the glass industry at three temperatures

T (°C)	Pb(II)		Cu(II)		Zn(II)	
	C_e	q_e	C_e	q_e	C_e	q_e
25	0.11	0.63	0.22	4.83	3.60	4.92
40	0.11	0.63	0.23	5.69	3.41	5.70
50	0.11	0.63	0.39	4.12	3.29	6.17

C_e (mg/L); q_e (mg/g).

The isotherm of Zn(II) at 40°C shows a plateau and therefore it is Langmuir type.

According to [23] k_F and n are Freundlich constants, the first one is proportional to adsorption capacity, a value of $1/n$ close to unity indicates favourable adsorption intensity, the values of $1/n$ for Cu(II) at 20°C, 40°C and 50°C were 0.75, 0.58 and 0.70 respectively and for Zn(II) were 0.44, 0.28 and 0.47 respectively, it can be considered that the interactions are weak between sorbate and adsorbent.

The Freundlich model indicates that the adsorption process occurs in multiple layers on an adsorbent surface [27,28]. For the wastewater from the glass industry, the adsorption capacities were determined at three temperatures (25°C, 40°C and 50°C) and equilibrium time of 2 h, it was determined from kinetics studies. The results for wastewater (Table 7) showed a similar trend for the adsorption capacities of Cu(II) and Zn(II) with the multicomponent solution (Table 6), the adsorption capacity increases from 25°C to 40°C, however the it decreases from 40°C to 50°C.

5. Conclusions

The main functional groups of the AL-PVA beads were identify by FTIR and it was found that hydroxyl group plays an important role on the removal of the ions, the SEM analysis showed that the composition of the beads significantly influences the roughness and porosity of material, and the EDS analysis confirmed the presence of the adsorbed cations, as well as the presence of calcium, $CaCl_2$ was added for the formation of the beads.

The swelling kinetics was of utmost importance for choosing the material, as well as the removal capacities at set conditions for each material. The results indicated that the best ratio was 3 (50/50). The acid stability shows that the AL/PVA beads are not stable at pH 1 and 2 due to weight loss, so it is recommended to work at pH higher than 4. The pH-zpc helped to determine the optimum pH (5.5) to perform the adsorption tests in the batch system. The removal percentage for each heavy metal was lower from wastewater from the glass industry than multicomponent solution, this due to the different initial concentrations (Pb(II) 0.18 mg/L, Cu(II) 1.72, Zn(II) 4.63 mg/L) of each ion and the competition between them.

The kinetics studies show that the optimum adsorption time was 8 h, in addition the kinetics data were best adjusted to the pseudo-first-order model indicating physisorption. The isotherms data were best adjusted to the linear model for Pb(II) and for Cu(II) and Zn(II) to the Freundlich model.

Conflict of interest

The authors declare that they have no conflict of interest.

References

[1] W. Vogel, Glass Chemistry, 2014.
[2] V. Kumar, Impact of glass industry effluent disposal on soil characteristics in Haridwar region, India, J. Environ. Health Sci., 2 (2016) 1–10.
[3] Z. He, J. Shentu, X. Yang, V. Baligar, T. Zhang, P. Stoffella, Heavy metal contamination of soils: sources, indicators and assessment, J. Environ. Ind., 9 (2015) 17–18.
[4] S. Rajeshkumar, Y. Liu, X. Zhang, B. Ravikumar, G. Bai, X. Li, Studies on seasonal pollution of heavy metals in water, sediment, fish and oyster from the Meiliang Bay of Taihu Lake in China, Chemosphere, 191 (2018) 626–638.
[5] M. Rabiul Awual, An efficient composite material for selective lead(II) monitoring and removal from wastewater, J. Environ. Chem. Eng., 7 (2019) 103087, doi: 10.1016/j.jece.2019.103087.
[6] A.A. Alghamdi, A.-B. Al-Odayni, W.S. Saeed, A. Al-Kahtani, F.A. Alharthi, T. Aouak, Efficient adsorption of lead(II) from aqueous phase solutions using polypyrrole-based activated carbon, Materials (Basel), 12 (2019) 2020, doi: 10.3390/ma12122020.
[7] E. Nassef, Y. Taweel, Removal of copper from wastewater by cementation from simulated leach liquors, J. Chem. Eng. Process Technol., 6 (2015) 1–6, doi: 10.4172/2157-7048.1000214.
[8] H. Hu, X. Li, P. Huang, Q. Zhang, W. Yuan, Efficient removal of copper from wastewater by using mechanically activated calcium carbonate, J. Environ. Manage., 203 (2017) 1–7.
[9] M. Maares, H. Haase, A guide to human zinc absorption: general overview and recent advances of in vitro intestinal models, Nutrients, 12 (2020) 762, doi: 10.3390/nu12030762.
[10] C. Jain, D. Singhal, M. Sharma, Adsorption of zinc on bed sediment of River Hindon: adsorption models and kinetics, J. Hazard. Mater., 114 (2004) 231–239.
[11] A. Abdolali, W. Guo, H. Ngo, S. Chen, N. Nguyen, K. Tung, Typical lignocellulosic wastes and by-products for biosorption process in water and wastewater treatment: a critical review, Bioresour. Technol., 160 (2014) 57–66.

[12] L. Largitte, R. Pasquier, A review of the kinetics adsorption models and their application to the adsorption of lead by an activated carbon, Chem. Eng. Res. Des., 109 (2016) 495–504.

[13] R. Karthik, S. Meenakshi, Removal of Cr(VI) ions by adsorption onto sodium alginate-polyaniline nanofibers, Int. J. Biol. Macromol., 72 (2015) 711–717.

[14] P. Cazón, M. Vázquez, G. Velázquez, Composite films of regenerate cellulose with chitosan and polyvinyl alcohol: evaluation of water adsorption, mechanical and optical properties, Int. J. Biol. Macromol., 117 (2018) 235–246.

[15] N. Delgado, A. Capparelli, A. Navarro, D. Marino, Pharmaceutical emerging pollutants removal from water using powdered activated carbon: study of kinetics and adsorption equilibrium, J. Environ. Manage., 236 (2019) 301–308.

[16] K. Kumeta, I. Nagashima, S. Matsui, K. Mizoguchi, Crosslinking of poly(vinyl alcohol) via bis(-hydroxyethyl) sulfone, Polym. J., 36 (2004) 472–477.

[17] A. Alshameri, H. He, J. Zhu, Y. Xi, R. Zhu, L. Ma, Q. Tao, Adsorption of ammonium by different natural clay minerals: characterization, kinetics and adsorption isotherms, Appl. Clay Sci., 159 (2017) 83–93.

[18] H. Moussout, H. Ahlafi, M. Aazza, H. Maghat, Critical of linear and nonlinear equations of pseudo-first-order and pseudo-second-order kinetic models, Karbala Int. J. Mod. Sci., 4 (2018) 244–254.

[19] H. Isawi, Using zeolite/polyvinyl alcohol/sodium alginate nanocomposite beads for removal of some heavy metals from wastewater, Arabian J. Chem., 13 (2020) 5691–5716.

[20] S. De, N. Aluru, B. Johnson, W. Crone, D. Beebe, J. Moore, Equilibrium swelling and kinetics of pH-responsive hydrogels: models, experiments, and simulations, J. Microelectromech. Syst., 11 (2002) 544–555.

[21] E. Bary, A. Fekri, Y. Soliman, A. Harmal, Characterisation and swelling-deswelling properties of superabsorbent membranes made of PVA and cellulose nanocrystals, Int. J. Environ. Stud., 76 (2018) 118–135.

[22] G. Tan, H. Yuan, Y. Liu, D. Xiao, Removal of lead from aqueous solution with native and chemically modified corncobs, J. Hazard. Mater., 174 (2010) 740–745.

[23] Y. Xiaofeng, F. Sun, Z. Han, F. Han, J. He, M. Ou, J. Gu, X. Xu, Graphene oxide encapsulated polyvinyl alcohol/sodium alginate hydrogel microspheres for Cu(II) and U(VI) removal, Ecotoxicol. Environ. Saf., 158 (2018) 309–318.

[24] E. Worch, Adsorption Technology in Water Treatment: Fundamentals, Processes, and Modeling, Walter de Gruyter GmbH and Co. KG, Berlin/Boston, Printed in Germany, 2012.

[25] F.A. Amaringo Villa, Determinación del punto de carga cero y punto isoeléctrico de dos residuos agrícolas y su aplicación en la remoción de colorantes, Rev. Invest. Agr. y Amb. 4 (2013).

[26] L. Li, F. Liu, X. Jing, P. Ling, A. Li, Displacement mechanism of binary competitive adsorption for aqueous divalent metal ions onto a novel IDA-chelating resin: isotherm and kinetic modeling, Water Res., 45 (2011) 1177–1188.

[27] J. Febrianto, A.N. Kosasih, J. Sunarso, Y.-H. Ju, N. Indraswati, S. Ismadji, Equilibrium and kinetic studies in adsorption of heavy metals using biosorbent: a summary of recent studies, J. Hazard. Mater., 162 (2009) 616–645.

[28] M. Moyo, L. Chikazaza, B.C. Nyamunda, U. Guyo, Adsorption batch studies on the removal of Pb(II) using maize tassel based activated carbon, J. Chem., 2013 (2013) 508934, doi: 10.1155/2013/508934.